

New ion trap for frequency standard applications

J. D. Prestage, G. J. Dick, and L. Maleki

California Institute of Technology, Jet Propulsion Laboratory, 4800 Oak Grove Drive, Pasadena, California 91109

(Received 3 February 1989; accepted for publication 10 April 1989)

We have designed a novel linear ion trap which permits storage of a large number of ions with reduced susceptibility to the second-order Doppler effect caused by the rf confining fields. This new trap should store about 20 times the number of ions as a conventional rf trap with no corresponding increase in second-order Doppler shift from the confining field. In addition the sensitivity of this shift to trapping parameters, i.e., rf voltage, rf frequency, and trap size, is greatly reduced.

INTRODUCTION

There has been much recent activity directed toward the development of trapped ion frequency standards, in part because ions confined in an electromagnetic trap are subjected to very small perturbations of their atomic energy levels. The inherent immunity to environmental changes that is afforded by suitably chosen ions suspended in dc or rf quadrupole traps has led to the development of frequency standards with very good long term stability.¹ Indeed, the trapped $^{199}\text{Hg}^+$ ion clock of Ref. 2 is the most stable clock yet developed for averaging times $\geq 10^6$ s. However, certain applications such as millisecond pulsar timing³ and low frequency gravity wave detection across the solar system⁴ require stabilities beyond that of present day standards.

While the basic performance of the ion frequency source depends fundamentally on the number of ions in the trap, the largest source of frequency offset stems from the motion of the atoms caused by the trapping fields via the second-order Doppler or relativistic time dilation effect.⁵ Moreover, instability in certain trapping parameters, e.g., trap field strength, temperature, and the actual number of trapped particles will influence the frequency shift and lead to frequency instabilities. Since this offset also depends strongly on the number of ions, a trade-off situation results, where fewer ions are trapped in order to reduce the (relatively) large frequency offset which would otherwise result.

We have designed and constructed a hybrid rf/dc linear ion trap which should allow an increase in the stored ion number with no corresponding increase in second-order Doppler instabilities. The 20 times larger ion storage capacity should improve clock performance substantially. Alternatively, the Doppler shift from the trapping fields may be reduced by a factor of 10 below comparably loaded hyperbolic traps.

SECOND-ORDER DOPPLER SHIFT FOR IONS IN A rf TRAP

Trapping forces in a rf ion trap are due to time-varying electric fields which increase in every direction from the trap's center. A single particle at rest in such a trap at its very center (where, in an ideal trap, these fields are zero) would have no velocity and thus no second-order Doppler shift.

A very different condition holds for many particles in such a trap. In this case, electrostatic repulsion tends to keep

the ions away from each other and from the center of the trap. As the number of ions increases, the size of the cloud also increases, pushing the ions into regions of larger and larger rf fields. The resultant velocity gives rise to a downward shift of atomic transition frequencies with increasing ion number.

Calculation of the second order Doppler shift requires a detailed knowledge of the ionic distribution density which results from the balance between trapping and (repulsive) Coulomb forces. A method has been developed in which an average over one cycle of the rf field reduces its effect to that of a pseudopotential acting on the charge of the particle.⁶ The effect is subsequently further reduced to that of a pseudocharge distribution which produces the equivalent effective potential. Ionic distribution density is then calculated by considering the response of charges to this resultant "background" pseudocharge.

This method has been previously applied⁷ to the trap shown in Fig. 1. Calculation shows a spatially uniform pseudocharge giving rise to a spherical ion cloud, also with uniform density. The resulting average frequency shift can be expressed in terms of the total number of trapped ions, together with a trap strength parameter ω , ion mass m , and charge q .

In the following sections we perform a similar calculation for a cylindrical geometry, a case not previously exam-

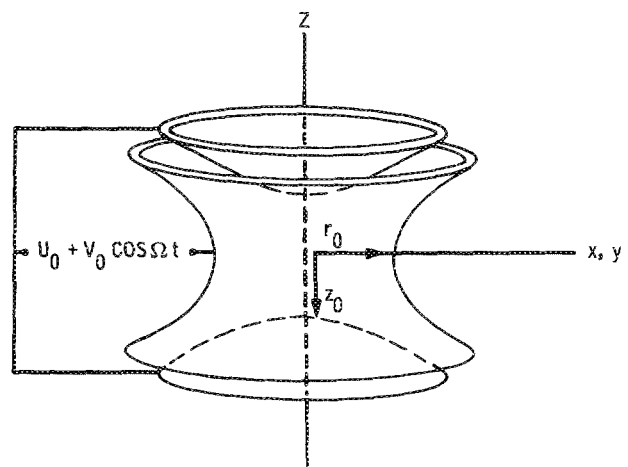


FIG. 1. A conventional hyperbolic rf ion trap. A node of the rf and dc fields is produced at the origin of the coordinate system shown.

ined. The cloud forms a cylinder of uniform density,⁸ in a manner analogous to that of the spherical trap. Comparison between the consequences of the two geometries shows a very different story. While physically similar in overall size, the linear trap can hold many more ions than the spherical one with no increase in the second-order Doppler shift, or conversely, the shift can be greatly reduced. Furthermore, its dependence on trap parameters is qualitatively different, allowing miniaturization of the transverse trap dimensions without penalty in performance.

CALCULATION FOR A SPHERICAL TRAP

Figure 1 shows a conventional rf ion trap along with the applied voltages. Trapping forces are generated by the driven motion of the ions (at frequency Ω) in an inhomogeneous rf electric field created by hyperbolic trap electrodes.⁶ The motion in each of three directions for a single ion in a rf trap is characterized by two frequencies, the fast driving frequency Ω and a slower secular frequency ω which is related to the harmonic force binding the particle to the trap center. An exact solution to the equations of motion shows that frequencies $k\Omega \pm \omega$, $k = 2, 3, \dots$ are also present. However, in the limit $\omega/\Omega \ll 1$ (which is the primary condition for stability of the ion orbits) the ω and $\Omega \pm \omega$ frequencies dominate and the kinetic energy (KE) of a particle, averaged over one cycle of Ω , separates into the kinetic energy of the secular motion and the kinetic energy of the driven motion. The average kinetic energy is transferred from the secular to the driven motion and back while the sum remains constant just as a harmonic oscillator transfers energy from kinetic to potential and back.

We consider two cases. A hot ion cloud, or one containing a very few ions where interactions between ions are negligible, shows a second-order Doppler shift given by

$$\left(\frac{\Delta f}{f}\right)_{\text{hot}} = -\frac{1}{2} \frac{\langle v^2 \rangle}{c^2} = -\frac{\langle \text{total KE} \rangle}{mc^2} \quad (1)$$

$$= -\frac{\langle \text{secular KE} + \text{driven KE} \rangle}{mc^2} \quad (2)$$

$$= -2(\langle \text{secular KE} \rangle / mc^2) \quad (3)$$

$$= -3k_B T / mc^2, \quad (4)$$

where m is the ionic mass, T the temperature, and $\langle \rangle$ indicates a time average over one cycle of Ω . We have also averaged over one cycle of ω to equate the secular and driven KE. This is analogous to a simple harmonic oscillator where the average KE is equal to the average potential energy. The consequence is a frequency shift that is twice as large as that due to thermal motion alone.

Of greater interest is the case where many ions are contained in a trap and interactions between ions dominate. In this cold cloud model⁷ displacements of individual ions from the trap center are primarily due to electrostatic repulsion between the ions, and random thermal velocities associated with temperature can be assumed to be small compared to driven motion due to the trap fields.

The electric potential inside the trap of Fig. 1 is

$$\phi(\rho, z) = \{[U_0 + V_0 \cos(\Omega t)]/\epsilon^2\}(\rho^2 - 2z^2), \quad (5)$$

where $\epsilon^2 = r_0^2 + 2z_0^2$ describes the trap size, and U_0 and V_0 represent the amplitudes of dc and ac trap voltages, respectively.

The trapping force generated by the rf field alone can be described by an electric pseudopotential⁶:

$$\psi(\rho, z) \equiv q[E_0(\rho, z)]^2/4m\Omega^2, \quad (6)$$

where q is the ionic charge and E_0 is the peak local rf field. This becomes

$$\psi(\rho, z) = (qV_0^2/m\Omega^2\epsilon^4)/(\rho^2 + 4z^2) \quad (7)$$

for the effect of the rf part of Eq. (5). Adding the dc potential from Eq. (5) gives the total potential energy for an ion in the trap of Fig. 1:

$$\phi(\rho, z) = \frac{1}{2}(m\omega_\rho^2\rho^2 + m\omega_z^2z^2), \quad (8)$$

where

$$\omega_\rho^2 = 2q^2V_0^2/m^2\Omega^2\epsilon^4 + 2qU_0/m\epsilon^2 \quad (9)$$

and

$$\omega_z^2 = 8q^2V_0^2/m^2\Omega^2\epsilon^4 - 4qU_0/m\epsilon^2 \quad (10)$$

describe secular frequencies for radial and longitudinal ion motion.

The pseudopotential can be further analyzed in terms of an effective pseudocharge by applying Poisson's equation to Eq. (7) or (8). The result of this calculation is a uniform background charge density throughout the trap region which is given by

$$Q_b = -[\epsilon_0 m(2\omega_\rho^2 + \omega_z^2)]/q. \quad (11)$$

An easy solution for the charge configuration can be found if we assume that the dc and rf voltages are adjusted to make the trapping forces spherical, i.e., $\omega_\rho = \omega_z = \omega$. In this case the ion cloud is also spherical and trapped positive ions exactly neutralize the negative background of charge, matching its density out to a radius where the supply of ions is depleted. Ion density is given by

$$n_0 = 3\epsilon_0 m\omega^2/q^2, \quad (12)$$

and the total number of ions by

$$N = n_0(4\pi/3)R_{\text{sph}}^3, \quad (13)$$

where R_{sph} is the radius of the sphere of trapped ions.

The oscillating electric field which generates the trapping force grows linearly with distance from the trap center. The corresponding amplitude of any ion's driven oscillation is proportional to the strength of the driving field, i.e., also increasing linearly with the distance from the trap center. The average square velocity of the driven motion for an ion at position (ρ, z) is

$$\langle v^2 \rangle = \frac{1}{2}\omega^2(\rho^2 + 4z^2). \quad (14)$$

For a given trapping strength, reflected in force constant ω^2 , the density is fixed by Eq. (12) while the radius of the spherical cloud is determined once the ion number N has been specified. The second-order Doppler shift due to the micromotion is found by taking a spatial average of Eq. (1) over the spherical ion cloud. Using Eq. (14) for the spatial dependence of the micromotion:

$$(\Delta f/f)_{\text{sph}} = -\frac{1}{2}(\overline{\langle v^2 \rangle}/c^2) \quad (15)$$

$$= -\frac{3}{10}(\omega^2 R_{\text{sph}}^2 / c^2) \quad (16)$$

$$= - (3/10c^2)(N\omega q^2/4\pi\epsilon_0 m)^{2/3}. \quad (17)$$

For typical operating conditions,⁷ $N = 2 \times 10^6$ and $\omega = (2\pi) 50$ kHz, $\Delta f/f = 2 \times 10^{-12}$. This second-order Doppler shift is about 10 times larger than the shift for free ¹⁹⁹Hg ions at room temperature, $\Delta f/f = 3k_B T / 2mc^2 = 2 \times 10^{-13}$.

If the temperature is not too high, its effect on the ion cloud is to broaden the sharp edge at its outside radius. In this case the plasma density falls off in a distance characterized by the Debye length⁸:

$$\lambda_D = \sqrt{k_B T \epsilon_0 / n_0 q^2}. \quad (18)$$

The cold cloud model should be useful provided the ion cloud size is large compared to the Debye length. This ratio is given by

$$\left(\frac{\lambda_D}{R_{\text{sph}}}\right)^2 = \frac{1}{30} \frac{(\Delta f/f)_{\text{hot}}}{(\Delta f/f)_{\text{sph}}}. \quad (19)$$

This indicates a relatively small fractional Debye length throughout the regime of interest. For the typical conditions indicated above, the Debye length is about 1/5 mm in comparison to a spherical cloud diameter of 2.5 mm.

CALCULATION FOR A LINEAR TRAP

For increased signal to noise in the measured atomic resonance used in frequency standard applications, it is desirable to have as many trapped ions as possible. However, as we have just seen, larger ion clouds have larger second-order Doppler shifts. This frequency offset must be stabilized to a high degree in order to prevent degradation of long term performance.

To reduce this susceptibility to second-order Doppler shift we now propose a hybrid rf/dc ion trap which replaces the single field node of the hyperbolic trap with a line of nodes. The rf electrode structure producing this line of nodes of the rf field is shown in Fig. 2. Ions are trapped in the radial

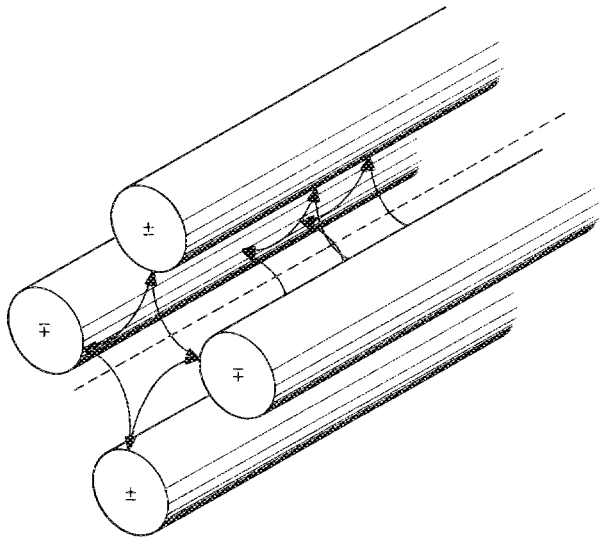


FIG. 2. The rf electrodes for a linear ion trap. Ions are trapped around the line of nodes of the rf field with reduced susceptibility to second-order Doppler frequency shift.

direction by the same type of rf trapping forces used in the previously discussed hyperbolic trap and we follow a similar analysis in terms of an equivalent pseudopotential and background pseudocharge.

Ions are prevented from escaping along the axis of the trap by dc biased "endcap" needle electrodes mounted on each end as shown in Fig. 3. These electrodes approximate the electrostatic effect of the missing parts of an infinitely long ion cloud. Their diameter is the same as the ion cloud to be trapped and is small compared to the trap diameter so that the rf trapping field is perturbed only slightly. Because these endcaps reach well inside the rf electrodes, any end effect of the rf fields on the ion cloud should be small. Unlike conventional rf traps this linear trap will hold positive or negative ions, but not both simultaneously.

Near the central axis of the trap we assume a quadrupolar rf electric potential:

$$\phi = [V_0(x^2 - y^2)\cos(\Omega t)]/2R^2, \quad (20)$$

from which, as in the previous section, we derive a corresponding pseudopotential:

$$\psi = (qV_0^2/4m\Omega^2 R^4)(x^2 + y^2), \quad (21)$$

for a total ionic potential given by

$$\phi = q\psi = m(\omega^2/2)\rho^2; \quad (22)$$

where, for the cylindrical electrodes of Fig. 2, R is an approximate distance from the trap center to an electrode's surface, and

$$\omega^2 = q^2 V_0^2 / 2m^2 \Omega^2 R^4. \quad (23)$$

Here ω is the characteristic frequency for transverse or radial motion in the trap. Longitudinal motion is described in terms of motion at thermal velocities between the trap ends.

Application of Poisson's equation shows Eq. (21) to be equivalent to a uniform background pseudocharge with density:

$$Q_b = - (2\epsilon_0 m \omega^2 / q). \quad (24)$$

Solving for the charge configuration for an infinitely long trap follows a nearly identical process to that of the preceding section since, from Gauss's law, cylindrical or spherical surfaces of charge induce no fields in their interior. Thus we find a uniform cylinder of ions just canceling the

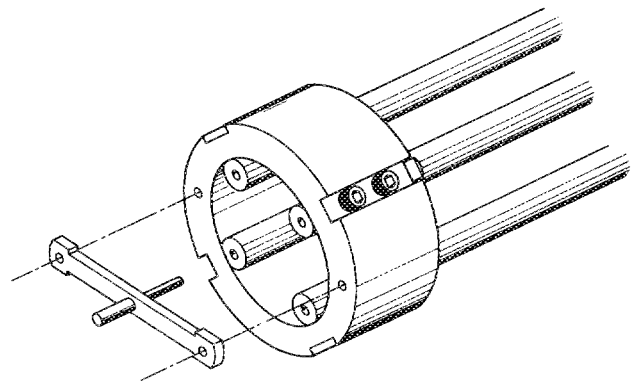


FIG. 3. The details of the dc endcap needle electrodes used to prevent ions from escaping along the longitudinal axis.

background pseudocharge out to a radius R_c with density:

$$n_0 = (2\epsilon_0 m \omega^2 / q^2), \quad (25)$$

with ion number per unit length of

$$N/L = n_0 \pi R_c^2. \quad (26)$$

The motion induced by the rf trapping field is purely transverse and is given by

$$\langle v^2 \rangle = \omega^2 \rho^2. \quad (27)$$

As before we average this quantity over the ion cloud to find the second-order Doppler shift:

$$\left(\frac{\Delta f}{f}\right)_{\text{lin}} = -\frac{1}{2} \frac{\langle v^2 \rangle}{c^2} = -\frac{\omega^2 R_c^2}{4c^2}. \quad (28)$$

We assume for simplicity a cylindrical ion cloud of radius R_c and length L . Equation (28) can be written in terms of total ion number N , and trap length L , as

$$\left(\frac{\Delta f}{f}\right)_{\text{lin}} = -\left(\frac{q^2}{8\pi\epsilon_0 mc^2}\right) \frac{N}{L}. \quad (29)$$

In contrast to the spherical case, this expression contains no dependence on trap parameters except for the linear ion density N/L . This is also true for the relative Debye length:

$$\left(\frac{\lambda_D}{R_c}\right)^2 = \frac{1}{24} \frac{(\Delta f/f)_{\text{hot}}}{(\Delta f/f)_{\text{lin}}}, \quad (30)$$

which must be small to insure the validity of our "cold cloud" model.

From this it is seen that the transverse dimension R of the trap may be reduced without penalty of performance, providing that operational parameters are appropriately scaled. This requires ω and Ω to vary as R^{-1} , and the applied voltage V_0 to be held constant.

COMPARISON

We can compare the second-order Doppler shift for the two traps assuming both hold the same number of ions by

$$\left(\frac{\Delta f}{f}\right)_{\text{lin}} = \frac{5}{3} \frac{R_{\text{sph}}}{L} \left(\frac{\Delta f}{f}\right)_{\text{sph}}. \quad (31)$$

As more ions are added to the linear trap their average second-order Doppler shift will increase. It will equal that of the spherical ion cloud in the hyperbolic trap when

$$N_{\text{lin}} = \frac{3}{5} (L/R_{\text{sph}}) N_{\text{sph}}. \quad (32)$$

A linear trap can thus store $\frac{3}{5}(L/R_{\text{sph}})$ times the ion number as a conventional rf trap with no increase in average second-order Doppler shift. For the trap we have designed, L is 75 mm. Taking $R_{\text{sph}} = 2.5$ mm for 2×10^6 $^{199}\text{Hg}^+$ ions in a spherical trap with similar overall size, we find that the linear trap capacity is about 18 times larger. Furthermore, it seems likely that the transverse dimension of the linear trap can be reduced to a value 100 or more times smaller than its length while maintaining constant ion number and second-order Doppler shift. This corresponds to a reduction in volume of 10 000 times.

DESIGN OF A LINEAR ION TRAP

We have designed a linear trap consisting of four molybdenum rods equally spaced on an approximately 1 cm radius. Axial confinement is accomplished by means of OFHC copper pins with dc bias which are located at each end and which are about 75 mm apart. The proximity of the four rods also aids axial confinement by localizing the coulomb interaction to an axial region with a length approximately equal to the trap's transverse dimension R . We calculate that a peak electrode potential of $V_0 = 180$ V at $\Omega = 2\pi$ 500 kHz is required to obtain a secular frequency $\omega = 2\pi$ 50 kHz.

The input optical system which performs state selection and also determines which hyperfine state the ions are in has been modified from the previous system.⁹ The present system illuminates about 1/3 of the 75-mm-long cylindrical ion cloud. An ion's room temperature thermal motion along the axis of the trap will give an average round trip time of 1.4 ms, a value which is much smaller than our optical pumping and interrogation times. Thus, during the time of the optical pulse all ions will be illuminated, and pumping and interrogation completed. The only change is that a somewhat longer optical pulse is required.

In order to operate within the Lamb-Dicke regime¹⁰ the 40.5-GHz microwave resonance radiation will be propagated perpendicular to the line of ions. The ions should then all experience phase variations of this radiation which are less than π so that the first-order Doppler absorption in sidebands induced by an ions motion will not degrade the 40.5-GHz fundamental.

The optical axis of the fluorescence collection system is perpendicular to the axis of the input optical system as in the previous system. There is one difference, however. In the hyperbolic trap the collection has in its field of view the ion cloud and the semitransparent mesh of both endcap trap electrodes. This mesh can scatter stray light into the collection system which will degrade the signal-to-noise ratio in the clock resonance. This linear trap has no trap electrodes, mesh or otherwise, in its field of view and, consequently, should have less detected stray light, allowing further performance improvement over the spherical trap.

CONCLUSIONS

Trapped ion frequency standards eliminate containing walls and their associated perturbations of the atomic transition frequencies by using electromagnetic fields alone to confine the particles. For any given trap, however, there exists a tradeoff between the number of ions in the trap and a frequency shift due to second-order Doppler effects. This tradeoff directly affects performance of the standard since the frequency shift is typically very much larger than the ultimate stability required and since the statistical limit to performance is directly related to ion number. We have calculated this performance tradeoff for a rf trap with cylindrical geometry, a case not previously considered for a trapped ion frequency source.

By replacing the single node in the rf trapping field for a spherical trap by a line of nodes, a cylindrical trap effectively increases effective volume without increasing overall size. Furthermore, this performance is found to be independent of

its transverse dimensions, as long as the driving frequency is scaled appropriately, with the driving voltage unchanged. More specifically, for the same frequency shift, we find that a linear trap with length L can hold as many ions as a spherical trap with diameter $6L/5$. In addition to the practical advantage of greatly reduced overall volume, a fundamental advantage is also allowed since operation within the Lamb-Dicke regime places a limit on the size of the ion cloud, a requirement which may be met for a cylindrical trap by irradiating the microwave atomic transition in a direction perpendicular to the trap's longitudinal axis.

We have designed a trapped ion frequency source in which a cylindrical trap is implemented with a combination of rf and dc electric fields. With similar overall size and improved optical performance, this trap has 15 to 20 times the ion storage volume as conventional rf traps with no increase in second-order Doppler shift.

ACKNOWLEDGMENTS

We wish to thank Dave Seidel for assisting in the design of the linear trap described here and G. R. Janik for helpful comments. This work represents the results of one phase of research carried out at the Jet Propulsion Laboratory, Cali-

fornia Institute of Technology, under contract sponsored by the National Aeronautics and Space Administration.

¹D. W. Allan, in *Proceedings of the 19th Annual Precise Time and Time Interval Applications and Planning Meeting*, edited by R. L. Sydner (U.S. Naval Observatory, Washington, DC, 1987), p. 375.

²L. S. Cutler, R. P. Giffard, P. J. Wheeler, and G. M. R. Winkler, *Proceedings of the 41st Annual Symposium Frequency Control*, IEEE Cat. No. 87CH2427-3, 12 (1987).

³L. A. Rawley, J. H. Taylor, M. M. Davis, and D. W. Allan, *Science* **238**, 761 (1987).

⁴J. W. Armstrong, F. B. Estabrook, and H. D. Wahlquist, *Astrophys. J.* **318**, 536 (1987).

⁵rf and Penning traps are both subject to second-order Doppler problems related to the trapping fields. In this paper we confine our attention specifically to the case of rf traps. We simply note that, for the same number of stored ions, magnetron rotation of the ion cloud in a Penning trap leads to a second-order Doppler shift of comparable magnitude to that for a rf trap. A Penning trap based clock is described in: J. J. Bollinger, J. D. Prestage, W. M. Itano, and D. J. Wineland, *Phys. Rev. Lett.* **54**, 1000 (1985).

⁶H. G. Dehmelt, *Adv. At. Mol. Phys.* **3**, 53 (1967).

⁷L. S. Cutler, R. P. Giffard, and M. D. McGuire, *Appl. Phys. B* **36**, 137 (1985).

⁸S. S. Prasad and T. M. O'Neil, *Phys. Fluids* **22**, 278 (1979).

⁹J. D. Prestage, G. J. Dick, and L. Maleki, in *Proceedings of the 19th Annual Precise Time and Time Interval Applications and Planning Meeting*, edited by R. L. Sydner (U.S. Naval Observatory, Washington, DC, 1987), p. 285.

¹⁰R. H. Dicke, *Phys. Rev.* **89**, 472 (1953).